Induction of nutrients into the mixed layer and maintenance of high latitude productivity

Richard G. Williams[1], Vassil Roussenov[1] and Michael J. Follows[2]

1. Department of Earth and Ocean Sciences, University of Liverpool, Liverpool, L69 3GP, UK

2. Program in Atmospheres, Oceans and Climate, Department of Earth Atmosphere and Planetary Sciences, Massachusetts Institute of Technology, Cambridge, USA

Submitted to *Global Biogeochemical Cycles*

July 14, 2005

Abstract

Nutrients are transferred from the nutricline into the winter mixed layer through a combination of vertical and lateral advection, referred to as induction, the reverse of the subduction process. This advective supply of nutrients maintains the high productivity at high latitudes over long timescales. Climatological diagnostics over the North Atlantic reveal that the induction of nutrients into the winter mixed layer is dominated by the lateral advection component even in the subpolar gyre where there is significant Ekman upwelling. The induction flux of nutrients is itself sustained by the strong nutrient transport associated with the western boundary currents, or nutrient streams. In the North Atlantic basin, the integrated induction flux accounts for nearly half the nitrate flux in the nutrient stream at 36°N, while the remaining fraction is recirculated in the thermocline of the subtropical gyre. The relationship between the nutrient stream and induction flux is illustrated using a numerical model of the circulation and biogeochemistry of the North Atlantic. The model studies suggest that the nutrient stream preferentially supplies nutrients to isopycnals outcropping in the subpolar gyre. The nutrient sources for the nutrient stream are either mode waters originating from the Southern Ocean or the tropics, where the eastern upwelling circulation and particle fallout focuses nutrients onto the lighter isopycnal surfaces of the nutrient stream.

1. Introduction

Basin-scale patterns of biological production are often explained in terms of the vertical transfer processes supplying nutrients, principally through convection and vertical upwelling. However, *Pelegri and Csanady* [1991] and *Pelegri et al.* [1996] have emphasized how boundary currents provide a crucial transport of nutrients within ocean basins which sustain the levels of biological production at high latitudes. They highlighted how the boundary currents lead to a 'nutrient stream', a plume of a high nutrient flux , vN, where v is the velocity along the boundary current and N is nutrient concentration. While the velocity of the boundary current is a maximum at the surface, the nutrient flux is a maximum below the surface, since the surface concentrations of inorganic nutrients are often low or exhausted over the subtropical gyre (Fig. 1a,b). The nitrate flux integrated across the cross-sectional area of the Gulf Stream increases by a factor of 3 from Florida Strait (24°N) to 36°N, reaching 677 kmol s^{-1} for waters lighter than $\sigma = 27.5$, then decreases downstream with typically half of the nutrient stream passing into the subpolar gyre and half recirculating within the subtropical gyre [*Pelegri et al.*, 1996].

In this study, we seek to complement the studies of *Pelegri and Csanady* by addressing the following questions: What is the mechanism by which nutrients carried in the stream are transferred downstream into the euphotic zone? What fraction of the nutrient stream flux is transferred into the sunlit surface waters? What is the upstream source of the nutrients in the stream?

The mechanism by which the nutrients in the stream are transferred to the surface is explored through climatological diagnostics of the subduction or induction process (Section 2). The relationship of the induction process to the nutrient stream is identified by comparing their nitrate fluxes within different density classes. The pathways of the nutrient stream and its effect on the large-scale productivity of the North Atlantic is addressed by using a coupled isopycnic circulation model and a simplified nitrate and dissolved organic nitrogen model (Section 3). The formation of the nutrient stream and the relative importance of tropical and Southern Ocean nutrient sources is examined in observed nutrient and tracer distributions and with the use of idealised model experiments (Section 4). Finally, there is a discussion of how the nutrient pathways and induction process regulate the gyre and basin-scale patterns of productivity over the Atlantic (Section 5).

2. Nutrient Streams and the Induction process

The nutrient stream only influences the export production when the nutrients are supplied to the euphotic zone. Given that the nutrient stream is a sub-surface feature at 36°N, this downstream supply of nutrients involves a two stage process. Firstly, the nutrients have to be transferred from the nutrient stream into the winter mixed layer, through the reverse of the subduction process and referred to here as ‘induction’, and secondly, the nutrients have to be transferred within the seasonal boundary layer via convection to the euphotic zone (Fig. 2).

In our view, the rate limiting process determining the annual supply of nutrients to the euphotic zone is the induction process, the transfer of nutrients into the winter mixed layer and seasonal boundary layer, while the subsequent seasonal cycle of the mixed layer dictates the timing of any peaks in productivity, such as the spring or autumn blooms.

2.1 Climatological view of the end of winter conditions

The instantaneous mixed layer distribution is highly variable in time through the diurnal and seasonal cycles in surface forcing, and the passage of synoptic-scale weather systems, as well as highly variable in space through stratification changes linked with ocean mesoscale eddy and frontal features. In order to provide a large-scale context for the nutrient transfer process, it is useful to define an interface marking the extent of the seasonal boundary layer by the thickness of the mixed layer at the end of winter. This end of winter interface is viewed as the maximum extent of the convection process. The end of winter mixed-layer distribution is diagnosed over the North Atlantic from climatological density profiles, defined by the depth where the potential density has decreased by 0.125 kg m^{-3} from the surface density. The end of winter mixed layer is characterized by a thickness of 50 m over the tropics, increasing polewards to 200 m over the northern flank of the subtropical gyre, then increasing to more than 300 m following a cyclonic circuit of the subpolar gyre (Fig. 3a,d). Concomitant with the polewards thickening of the mixed layer, there is an increase in the mixed-layer density from less than $\sigma_\theta = 24.0$ in the tropics, reaching between $\sigma_\theta = 26.75$ and 27.0 over the subtropical/subpolar boundary and increasing further to $\sigma_\theta = 27.5$ in the northwest corner of the subpolar gyre (Fig. 3b). This polewards thickening of the mixed layer is also associated with an increase in the nitrate concentration, which ranges from 0.5 to 2μM over the subtropical gyre and increases to between 4 to 12μM (M$\equiv$mol l^{-1}) over the subpolar gyre (Fig. 3c); also see similar maps for the mixed-layer nitrate concentrations by *Glover and Brewer* [1988]. The transfer of these nutrients by convection and the wind-driven Ekman transfer has previously been discussed by *Williams et al.* [2000] and *Williams and Follows* [1998] respectively. While convection redistributes the nutrients within the mixed layer, this process cannot sustain the nutrient concentrations within the seasonal boundary layer over several annual cycles if there is an export flux through the base of the winter mixed layer (as the convective flux by definition goes to zero at the base of the winter mixed layer). There has to be another mechanism to re-supply the nutrients within the seasonal boundary layer. While traditionally, this re-supply has been invoked in terms of a vertical diffusion or advection, instead we advocate the isopycnic transport of nutrients (as reviewed in *Williams and Follows* [2003]).

2.2 Annual rate of subduction and induction over the North Atlantic

The most important process in sustaining the end of winter nutrient concentrations in the mixed layer over a basin is the background gyre circulation, which involves both a vertical and horizontal transfer between the main thermocline and the end of winter mixed layer. The volume flux transferred from the seasonal boundary layer into the main thermocline is defined by the subduction rate (Fig. 2a) [*Marshall et al.*, 1993], which for climatological diagnostics can be evaluated as

$$S_{ann} = -w_H - \mathbf{u}_H \cdot \nabla H \tag{1}$$

where H defines the position of the interface given by the end of winter mixed layer, w

and $\mathbf{u}$ are the vertical velocity and horizontal velocity respectively at this interface. S_{ann} has units of m y^{-1}, but should be viewed as a volume flux per unit area, m^3 y^{-1}/m^2. A recent eddy-resolving model study of the subduction process is broadly supportive of these end of winter climatological diagnostics [*Valdiviesio da Costa et al.*, 2005], although they highlight how the stronger flows in the Gulf Stream lead to enhanced subduction rates there. The annual subduction rate is evaluated following *Marshall et al.* [1993], where full details are given. The horizontal velocity, $\mathbf{u}_H$, is evaluated assuming thermal-wind balance using the horizontal density gradients evaluated from the Levitus climatology assuming a reference level of 2.5 km or the sea floor if shallower (Fig. 3d). The horizontal volume flux directed across the end of winter interface is evaluated from the scalar product, $\mathbf{u}_H \cdot \nabla H$.

The vertical velocity at the base of the Ekman layer, w_{ek}, is evaluated from the annually-averaged surface winds from *Isemer and Hasse* [1981] climatology (Fig. 4a), then the vertical velocity at the interface $z = -H$ is evaluated using linear vorticity balance

$$w_H = w_{ek} - \frac{\beta}{f} \int_{z=-H}^{z=0} v dz, \qquad (2)$$

where f is the planetary vorticity, $\beta = df/dy$, and v is the meridional velocity.

Our focus is on the volume flux into the winter mixed layer, so we concentrate on $-S_{ann}$ (Fig. 4b). The climatological diagnostics reveal that the volume flux *into* the winter mixed layer is greater than 100 m y^{-1} over the Gulf Stream extension and over much of the subpolar gyre. In contrast, over much of the subtropical gyre, the volume flux is directed *from* the mixed layer into the main thermocline with S_{ann} reaching 100 m y^{-1} over the gyre recirculation, but elsewhere is more typically 50 m y^{-1}.

The intensity of the subduction rate is much greater than the vertical wind-induced Ekman transfer, which only reaches a maximum magnitude of 50 m y^{-1}, particularly over the Gulf Stream extension and recirculation, and over the subpolar gyre. In addition, the zero line of w_{ek} is much further north than that of S_{ann} due to the lateral transfer into the polewards thickening of the mixed layer.

2.3 Induction flux of nutrients into the winter mixed layer

The induction flux of nutrients into the winter mixed layer is given by the product of the volume flux per unit area into the end of winter mixed layer, $-S_{ann}$, and the nutrient concentration in the mixed layer at the end of winter, N_w:

$$-S_{ann}N_w. \tag{3}$$

This induction flux of nutrients has the same units as used for the nutrient stream, the product of a velocity and a nutrient concentration. Choosing N_w to be nitrate now, there is a high induction flux of nitrate into the mixed layer over the Gulf Stream extension and over the subpolar gyre (Fig. 4d), which is to be expected given the patterns of N_w and $-S_{ann}$ (Figs. 3c and 4b). Again this induction flux is much larger than the corresponding Ekman transfer, $w_{ek}N_w$, which only reaches comparable magnitudes over the northern flank of the subpolar gyre (Fig. 4c).

While the Ekman suction induced by the winds ultimately controls the deformation of the thermocline and gyre circulation, this suction does *not* directly provide the dominant supply of nitrate to the mixed layer or euphotic zone. Instead the nutrient concentrations in the end of winter mixed layer on the basin scale are sustained by the induction of nutrients from the gyre circulation. The induction flux of nutrients can be separated into the contributions from the vertical and horizontal transfer into the end of winter mixed layer (Fig. 5). The vertical transfer at the base of the winter mixed layer only makes a significant contribution to the induction flux in the tropics and on the northern flank of the subpolar gyre (Fig. 5a,b). In comparison, the horizontal contribution controls the high induction rates along the Gulf Stream and over much of the subpolar gyre (Fig. 5c,d).

These essential points hold even though the details of our diagnostics are sensitive to the choice of the climatological winds, background circulation and end of winter mixed-layer distribution.

2.4 Induction flux of nutrients and the Nutrient Stream

In our view, the induction flux of the nutrients is itself sustained by the nutrient stream (Fig. 2b). However, a fraction of the nutrient stream is not inducted into the mixed layer and instead recirculates within the subtropical thermocline. Hence, we expect that the nutrient flux in the stream to be comparable to, or greater than, the downstream induction into the seasonal boundary layer:

$$\int_{-D_o}^{0}\int_{x_1}^{x_2} vN dx dz \geq \int_{A} \left(-S_{ann}N_w\right) dx dy, \quad (4)$$

where the left hand integral is applied over the width of the boundary current from longitudes x_1 to x_2 and over the depth of isopycnals, D_o, that outcrop downstream within the basin, while the right hand integral is applied over the horizontal area over which the density layers in the nutrient stream outcrop. An exact balance in (4) would also only be possible if there is a steady state and diffusive transfers, as well as biological sources and sinks were unimportant. When the nutrients are fluxed into the winter mixed layer they may subsequently be redistributed onto other density layers through diabatic transfer in the mixed layer, supported by air-sea buoyancy fluxes, or biological consumption leading to a particle flux which is remineralised in different density layers.

Given this advective balance, it is useful to re-examine the mixed-layer winter distribution and nutrient stream diagnostics. The σ range of the dominant part of the nutrient stream is from $\sigma = 26.6$ to 27.4 (Fig. 1c), which outcrops into the winter mixed-layer over the northern part of the subtropical gyre and much of the subpolar gyre (Fig. 3b, dashed contours). Over the same outcrop region, there are elevated nitrate concentrations (Fig. 3c). Hence, the density class of the nutrient stream is in accord with the downstream nutrient distribution in the winter mixed layer.

The subduction and induction fluxes of volume and nitrate are now separately diagnosed within σ classes over the North Atlantic south of 60°N (Table 1). The subduction contributions are summed only when $S_{ann} > 0$ and, conversely, the induction contributions are summed when $S_{ann} < 0$ for each density class, which are chosen to be comparable with those reported by *Pelegri et al.* [1996]. Firstly, there is a relatively small subduction flux of volume and nitrate over the North Atlantic within the core of the nutrient stream, $26.5 \leq \sigma < 27.3$, reaching 8.4 Sv and 69 kmol s^{-1} (Table 1). This subduction process leads to the relatively depleted nutricline over the subtropical gyre [*Palter et al.*, 2005].

Secondly, there is a much larger induction flux of volume and nitrate within the core of the nutrient stream reaching 18.4 Sv and 188 kmol s^{-1} (Table 1). In comparison, *Pelegri et al.* [1996] diagnose a maximum volume flux of 29.2 Sv and an associated nitrate flux of 487 kmol s^{-1} within these same density classes passing through a section crossing the Gulf Stream at 36°N. The differences between the induction and nutrient stream estimates of the volume and nitrate fluxes are probably principally due to the nutrient stream diagnostics only being applied over a limited extent and, thus, include recirculating components, as well as our climatological diagnostics underestimating the circulation and induction flux. While our induction fluxes are smaller than that diagnosed by *Pelegri et al.* [1996], there is a broadly similar σ distribution with the maximum flux concentrated in the band from $26.8 \leq \sigma < 27.1$.

In order to explore the connection between the nutrient stream and downstream induction process in a more dynamically-consistent manner, we now examine the nutrient pathways within an isopycnic circulation model.

3. A model study of the downstream affect of the Nutrient Stream

3.1 Model formulation

The model study employs an isopycnic model (MICOM 2.7; *Bleck and Smith* [1990]) with a formulation similar to that employed by *Roussenov et al.* [2005]. The model includes 15 isopycnal layers in the vertical plus a surface mixed layer with variable density and a horizontal resolution of 1.4° on a Mercator grid (150 km at the equator and 75 km at 60°N). The model topography is based on ETOP05 data averaged within the model grid. There is a diapycnic diffusivity, $\kappa = 10^{-7}/N$, varying with buoyancy frequency N, which typically varies from 10^{-5} m^{2}s^{-1} in the thermocline to 10^{-4} m^{2}s^{-1} in the deep waters. In addition, the isopycnic model employs isopycnic mixing and thickness diffusion (using a diffusive velocity of 0.5 cm s^{-1} with Laplacian and biharmonic forms respectively), and deformation-dependent momentum mixing (using a mixing velocity of 1 cm s^{-1} with a background Laplacian dependence). The model is forced using monthly wind stress, surface freshwater fluxes, surface radiative fluxes, with latent and sensible heat fluxes calculated from air temperature and water vapour mixing ratio from ECMWF (ERA20). Rivers are added as freshwater fluxes at corresponding coastal grid points. The Strait of Gibraltar is closed, but the salinity of subsurface layers at this location is relaxed to climatology on a 30 day relaxation time scale. On the northern and southern boundaries, there is a 'sponge relaxation' to climatology (relaxation time scale increasing from 30 to 180 day) for temperature in the mixed layer, salinity and the height of density interfaces for all layers. The model is initialized from Levitus climatology (temperature, salinity and density) and integrated for an initial spin up of 60 years and then a further 40 years in an on-line coupled mode where nutrient or tracer experiments are conducted.

3.2 Nutrient cycling

The total nitrogen is separated into nitrate, dissolved organic nitrogen (DON) consisting of semi-labile and refractory components, and particulate organic nitrogen (PON). The PON is assumed to fallout and be remineralised in the interior with a vertical scale of 200 m, while the dissolved inorganic, semi-labile and refractory organic nutrients are assumed to be transported by the circulation with lifetimes in the euphotic zone of typically 6 months and 6-12 years respectively; see further details in the Appendix and a justification of the model closures in *Roussenov et al.* [2005].

The initial nitrate is taken from Levitus climatology (NODC), while the semi-labile DON is initialised to be 0 and the refractory DON initialised as 2 μM below 2 km and 4 μM above 2 km. On the open boundaries, the nutrients are continuously relaxed to the initial conditions within the buffer zones, and there are no atmospheric or riverine inputs of nutrients, or any loss of nutrients on the seafloor through burial. The nitrogen model is integrated for 40 years online after the 60 year dynamical spin up.

The model broadly captures the observed meridional structure of the nitrate distribution (Fig. 6a). There is a plume of high nitrate associated with the Antarctic Intermediate Water, passing into the domain from 20°S at depths from 500 m to 1500 m. In the data, the plume becomes diluted northwards of 20°N and eventually is not a distinct feature at higher latitudes. In the model, there is a similar dilution of the plume, but this weakening starts north of the equator. In deep waters below 500 m, the lowest nitrate concentrations are in the subpolar gyre, reflecting the relatively recent ventilation and low age there.

For maps of the annually-averaged, surface nitrate in the model and the climatological data, there is the expected northwards increase in nitrate concentrations associated with the thickening of the winter mixed layer over the North Atlantic (Fig. 6b). However, the model overestimates the surface nitrate by 1 to 3 μM over the North Atlantic, but at the same time underestimates the surface nitrate by up to 5 μM in the upwelling zones centred off Africa at 15°N and 20°S. This underestimate of the upwelling signal is probably due to using monthly-averaged wind forcing. Conversely, the model overestimate in the subtropical gyre might possibly be due to the background circulation being too weak and leading to the plume of nitrate-rich, Antarctic Intermediate water being advected insufficiently far north.

The modelled PON export ranges from 0.05 M m^{-2}y^{-1} over much of the tropical and subtropical Atlantic and increasing to 0.35 M m^{-2}y^{-1} over higher latitudes and the African upwelling zones centered at 20°N and 20°S (Fig. 6e). This pattern is broadly in accord with the adjoint model estimates of export production by *Usbeck et al.* [2003] where the model is constrained by nitrate observations and, to a lesser extent, sediment trap observations. The modelled DON over the euphotic zone has elevated concentrations in the tropics (10°S-5°N) with lower values at 20°S and 40°N (Fig. 6d); discussed and compared with data in *Roussenov et al.* [2005].

3.3 Modelled nutrient stream

The nutrient model is now used to consider how the nutrient stream is formed and its downstream effect. For reference, the depth-integrated transport has the classical anti-cyclonic circulation over the subtropical gyre (10°N to 40°-50°N) and cyclonic circulation over the subpolar gyre. The depth-integrated horizontal transport reaches 35 Sv (1 Sv=10^6m^{3}s^{-1}) over the Gulf Stream, which is consistent with the wind-stress curl forcing. There is not the observed enhancement of the boundary current transport to perhaps 100 Sv due to the relatively coarse horizontal resolution.

Flow trajectories are considered along the core of the nutrient stream on the $\sigma = 27.03$ surface, as seen in the data (Fig. 1c). Trajectories associated with the influx of nutrients in the Gulf Stream partly originate from south of the equator along the western boundary or in the tropical upwelling zones in the eastern Atlantic (Fig. 7, sites A to C). Trajectories leaving the Gulf Stream spread into both the subtropical and subpolar gyres (Fig. 7, site D) and, thus, provide a nutrient flux into both gyres, as argued by *Pelegri and Csanady* [1991]. Trajectories remaining within the subtropical gyre by definition eventually rejoin the Gulf Stream and can provide an additional nutrient flux to the boundary current. There are also recirculating trajectories within the subpolar gyre which circuit the northern North Atlantic through the cyclonic interior gyre circulation and the southwards Labrador Current (Fig. 7, site E). All these trajectories become more complex and include more recirculating components as the model resolution increases. However, they still provide a large-scale view of the relevant pathways upstream and downstream of the nutrient stream. This Lagrangian view is taken further in subsequent tracer release experiments.

In the model, the nitrate stream is revealed by a subsurface plume of high nitrate flux running northwards from the southern boundary along the western boundary, crossing the equator, and continuing to 36°N where the nitrate stream leaves the western boundary and crosses to the eastern side of the subpolar gyre (Fig. 7a, shaded). The core of the nutrient stream is along $\sigma = 27.03$, where a nitrate tongue extends northwards from the tropics through the western boundary advection (Fig. 7b).

Along 36°N, the model velocity section reaches 35 cm s^{-1} and there is an associated high nitrate flux centred at a depth of 500 m (Fig. 8a). In density space, the modeled nitrate stream has two maxima reaching 4 mM m^{-2}s^{-1}, located between $\sigma = 26.9$ to 27.3 (Fig. 8b, shaded). In comparison, the diagnostics of Pelegri and Csanady [1991] along 36°N reveal a higher nitrate flux of greater than 10 mM m^{-2}s^{-1} at slightly shallower depths from 250 m to 750 m and within a σ range of 26.7 to 27.2 (Fig. 1b,c). Associated with the nitrate stream, there is also a high DON flux reaching 2.5 mM m^{-2}s^{-1} concentrated within the upper 500 m and in the lighter range of $\sigma = 26.4$ to 26.7. The DON stream transfers high concentrations of DON in the tropics to higher latitudes within the North Atlantic (Fig. 8a). This signal is smaller than the modeled nitrate flux by a factor of 2, but still represents a potentially important nutrient pathway within the North Atlantic [*Rintoul and Wunsch*, 1991; *Mahaffey et al.*, 2004; *Roussenov et al.*, 2005].

The nutrient stream is revealed at 20°S by a plume of high nitrate flux along the western boundary, which stays confined to the western boundary to the equator (Fig. 8c). The nutrient strengthens in intensity across the equator and reaching a maximum at 36°N, reflecting the combination of the input of nutrient-rich waters and the strengthening of the boundary current, then weakens downstream (Fig. 7a, right panel). The nutrient stream crosses the North Atlantic, eventually leading to northwards plume on the eastern boundary of the subpolar gyre (Fig. 8c).

The model, at 1.4° resolution, underestimates the strength of the nutrient stream and makes the feature too deep by typically 100 m and too dense by 0.1 σ unit. While accepting these caveats concerning the realism of the model, we now conduct tracer experiments to reveal the downstream effect of the nutrient stream.

3.4 Downstream effect of the nutrient stream

In order to understand the influence of the nutrient stream, a coupled tracer and isopycnic model integration is conducted where an idealised tracer is released in selected layers in the region of the Gulf Stream. Tracers are released in two targeted layers denoting the lightest part of the nutrient stream, $\sigma = 26.52$, and the core of the nutrient stream,

$\sigma = 27.03$. Each tracer is released with a source value of 1 into a background value of 0, and each tracer integration is independent of each other with no mixing of the different tracers together. The tracer integrations are repeated for (i) a conserved tracer and (ii) for a tracer mimicking the cycling of nitrate with consumption in the euphotic zone, particle fallout and remineralisation at depth with a remineralisation depth scale of 200 m (in accord with the nitrate model described in the Appendix). The tracer spreading is tracked after 40 years online integration, after an initial dynamical spin up of 60 years.

Firstly, for the conserved tracer in the lightest layer, $\sigma = 26.52$, the tracer spreads over the subtropical gyre with greater concentrations close to the source region in the Gulf Stream (Fig. 9a, left panel). The tracer broadly remains within the subtropical gyre, but does spread northwards of the winter outcrop of the layer within the mixed layer. For the model integrations, the interior diapycnal transfer is relatively weak and so the tracer spreading is initially confined within the initial source layer (Fig. 9a, dashed lines). However, the tracer eventually spreads into the mixed layer where the layer outcrops. Within the mixed layer, there is diabatic forcing leading to the tracer being transferred to other density classes and eventually subducted into the thermocline within these neighbouring density classes (Fig. 9b; left panel). This transformation is more striking for the denser layer, $\sigma = 27.03$, where the tracer spreads over much of the upper thermocline in the subtropical gyre (Fig. 9c,d; left panel).

Secondly, for the nitrate-like tracer with a particle flux, the tracer spreads much further north from the Gulf Stream source region into the subpolar gyre (Fig. 9a,c, right panel). The inclusion of the particle flux and remineralisation leads to the tracer concentrations being greatly enhanced within the upper thermocline (Fig. 9b,d, right panel). The downstream induction process, transferring nutrients from the thermocline into the mixed layer, then leads to the much higher tracer concentrations over the mixed layer in the subpolar gyre. Conversely, there is less tracer spreading over the eastern-side of the subtropical gyre due to the consumption of the tracer within the euphotic zone (Fig. 9a, right panel). In summary, the nutrient stream directly affects the downstream nutrient concentrations within the mixed layer in both the subtropical and subpolar gyres. This downstream transfer occurs through the induction process, but this advective transfer is significantly augmented by the nitrate cycling leading to enhanced nitrate concentrations in denser layers outcropping in the subpolar gyre.

4. How are Nutrient Streams formed?

The nutrient streams are obviously related to the high velocities associated with the western boundary currents and their extensions into the gyre interior. However, the nutrient stream has a subsurface maximum that is dictated by the product of the nutrient and velocity profiles. We now consider where the nutrients associated with the nutrient stream originate from.

4.1 Nutrient source from the tropics or the Southern Ocean?

The transport pathways are now considered in terms of the PO_4^* tracer [*Broecker and Peng*, 1982],

$$PO_4^* = PO_4 + O_2/175, \tag{5}$$

which is conserved for biotic reactions following Redfield stoichiometry where the change in phosphate from remineralisation of organic fallout is compensated by the oxygen consumed. Along the $\sigma = 26.5$, 27.0 and 27.5 surfaces making up the nutrient stream, the PO_4^* tracer reveals source waters with highest concentrations in the mode waters originating from the Southern Ocean (Fig. 10, right panel). There is also a local maximum in the tracer concentration over the Labrador Sea in the northern subpolar gyre.

The nitrate distributions are now considered along the same σ surfaces (Fig. 10, left panel). Along the lighter surfaces, the highest nitrate concentrations are in the tropical upwelling zones off Africa centrered at 15°S reaching 25 μM and 35 μM along the $\sigma = 26.5$ and 27.0 surfaces respectively; also see *Hansell and Follows* [2005]. In contrast, on denser surfaces, the highest nitrate concentration are within the sub-Antarctic mode waters , reaching 32.5 μM in the South Atlantic along the $\sigma = 27.5$ surface.

The difference between the PO4* and nitrate distributions suggests that biotic processes lead to the elevated nitrate concentrations in the tropical Atlantic. The preferential enhancement of the nutrient concentrations on the lighter σ surfaces is a consequence of the remineralisation of the particulate fallout being concentrated over the upper few 100 m of the water column.

In summary, the data diagnostics suggest that the ultimate nutrient source for the nutrient stream are the intermediate waters from the Southern Ocean, as advocated by *Sarmiento et al.* [2004], together with a weaker possible contribution from high-latitude subpolar waters. However, biotic processes play an important role in locally enhancing the nutrient concentrations in the tropics. Along the lighter σ surfaces, this biotic cycling is sufficiently strong to focus the nutrients onto these surfaces and leading to the maximum nitrate concentrations occurring in the tropics, rather than in the formation regions for the water masses.

4.2 Model signals of the nutrient supply from a southern source

The large-scale competition between the advective transfer of nutrients and their biotic transformations is now explored again using idealised tracer experiments. A tracer source is included in the South Atlantic at 30°S along the western boundary within targeted isopycnal layers, $\sigma = 26.52$ and 27.03 (with each tracer release treated independently). The experiments are again conducted for a passive conserved tracer and for a tracer mimicking the cycling of nitrate, and integrated online for 40 years.

Firstly, for the conserved tracer, there is the northwards spreading with the expected decrease in tracer concentration away from the source in both layers (Fig. 11a). After 40 years, the tracer front is further north along a zonal band along 10°N for the lighter surface ($\sigma = 26.52$), whereas the front is inclined from the northwest to southeast across the equator for the denser surface ($\sigma = 27.03$).

Secondly, for the tracer mimicking nitrate, there are much higher concentrations in the tropics for the lighter surface (Fig. 11b). The tracer concentration reaches 10 times the source value in the eastern upwelling region of the tropics. The vertical cycling of the tracer leads to the tracer spending longer in the tropical upwelling zone where higher tracer concentrations are acquired from the remineralisation of the particle fallout through nutrient trapping [*Najjar et al.*, 1992]. There is little enhancement of the tracer concentrations for the $\sigma = 27.03$ source, since this layer is too deep to provide a tracer influx into the euphotic zone and drive a resulting particle flux. An important difference with the data is that the tracer integrations for different layers are treated independently. Thus, the model experiments do not include the process by which nitrate supplied by lighter layers to the euphotic zone can enhance the nitrate concentrations in the underlying denser layers by fueling export production and leading to remineralisation of the particle flux.

Thus, our interpretation of the isopycnal nitrate distributions in the data (Fig. 10) is as follows: (i) the tropical enhancement along $\sigma = 26.5$ results from the recycling of fallout due to the nitrate influx into the euphotic zone from that layer; (ii) the enhancement along $\sigma = 27.0$ is a result of recycling of fallout from a nitrate influx into the euphotic zone from lighter layers; and (iii) the lack of any tropical enhancement of nitrate along $\sigma = 27.5$ is due to this layer being too deep to experience significant remineralisation. Thus, the localization of the nutrient maximum along a σ surface is either in the tropics when significant remineralisation is experienced or is in the Southern Ocean mode waters.

5. Discussion

Export production over the basin scale requires a nutrient supply to the euphotic zone to offset the loss of nutrients from organic fallout. Over a seasonal timescale, convection can often provide much of this necessary flux. However, convection only redistributes nutrients within the seasonal boundary layer. Again, if there is particulate fallout from this seasonal boundary layer, then there has to be a compensating influx of nutrients to sustain the patterns of export production.

Over much of the basin circulation, this advective supply of nutrients is achieved through a combination of the nutrient streams, sub-surface plumes of high nitrate flux, and the subsequent, downstream transfer into the seasonal boundary layer (Fig. 12a). The nutrient streams provide an influx of nutrients into both the subtropical and subpolar gyres, as first illustrated by *Pelegri and Csanady* [1991]. The subsequent advective transfer of nutrients into the seasonal boundary layer is provided by the induction process, the reverse of the subduction process that determines the interior water-mass distributions. Our climatological diagnostics suggest that the induction of nutrients into the seasonal boundary layer is achieved by an isopycnal transfer into a mixed layer, which is a consequence of the mixed layer becoming denser and thicker downstream following a cyclonic circuit of the subpolar gyre from the Gulf Stream to the Labrador Sea. Over the core of the nutrient stream, nearly half the nutrient flux associated with the boundary current at 36°N is transferred into the winter mixed layer, while the remainder is probably recirculated. This advective input of nutrients acts to sustain the patterns of export production over the subpolar gyre. In regions where macro nutrients are not limiting, then the nutrients might ultimately be subducted through mode water formation and be returned southwards as part of the overturning circulation.

Over the oligotrophic subtropical gyres, the large-scale circulation only provides a nutrient influx into the mixed layer close to the Gulf Stream recirculation. More generally, fluid is subducted from the mixed layer into the underlying thermocline, as reflected in low nutrient concentrations in 18^{o}C mode water being transferred into the upper thermocline [*Palter et al.*, 2005]. This transfer leads to the classical problem of how export production is sustained over the subtropical gyres. On the flanks of the gyres, there can still be a surface lateral transfer through a combination of the horizontal Ekman flow and eddy, down-gradient transfers [*Williams and Follows*, 1998]. In the central part of the gyre, export production might be sustained through a vertical transfer through diapycnic processes [*Pelegri and Csanady*, 1994; *Jenkins and Doney*, 2003] or eddy transfer processes [*McGillicuddy et al.*, 1998]. Alternatively, nitrogen fixation [*Gruber and Sarmiento,* 1997] or consumption of semi-labile DON might provide comparable contributions [*Rintoul and Wunsch*, 1991; *Roussenov et al.*, 2005].

On the larger basin scale of the Atlantic, the nutrient pathways reflect an interplay of the nutrient sources in the mixed layer and the circulations associated with the gyre, intermediate and, ultimately, the deep waters (Fig. 12b). Nutrients transported in these different layers are connected through the particle flux providing a vertical transfer of nutrients, which can form local maxima in the nutrient concentrations within an isopycnal layer. For the Atlantic, there is an influx of nutrients from the Southern Ocean linked to the transport of sub-Antarctic mode water, as recently emphasized by *Sarmiento et al.* [2004]. The sub-Antarctic mode water is probably formed north of the polar front, probably preferentially in the Indian Ocean, and then swept by the Agulhas Current and gyre circulation northwards over the South Atlantic [*Rintoul*, 2005]. In the tropics, the upwelling leads to a local enhancement of the nitrate concentrations through the remineralisation of the particulate fallout. A combination of the nutrient-rich AAIW and the tropical waters are then swept northwards through the gyre circulation along the western boundary of the northern subtropical gyre. This nutrient stream is then swept over the rest of the basin.

While the eddy and frontal circulations are important in locally enhancing export production, they play a less significant role for the basin-scale transport of nutrients. The eddies probably are more significant at gyre boundaries in providing a down-gradient diffusive transfer along density surfaces. However, in our view, the basin-scale patterns of export production are more controlled by the pathway of the nutrient streams reflecting the boundary currents and the advective transfer into the winter mixed layer.

Our view has emphasized a climatologically-averaged picture. However, the subduction and induction process is dependent on the thickness of the winter mixed layer, which varies year on year according to the buoyancy loss to the atmosphere and the background stratification. Consequently, interannual and decadal variations in the induction process are to be expected. This temporal variability will then accordingly lead to changes in surface nutrient concentrations and, if the nutrients are limiting, variations in export production.

Acknowledgements. The work was supported by a NERC 36N Consortium grant

(NER/O/S/2003/00625).

APPENDIX: Nitrate and DON model

The evolution of nitrate, semi-labile DON and refractory DON are given by

$$\frac{\partial}{\partial t}\mathrm{NO}_3^- + \nabla\cdot(\mathbf{u}\mathrm{NO}_3^-) = F_{NO3} \tag{A1}$$

$$\frac{\partial}{\partial t}(\mathrm{DON}_s + \mathrm{DON}_r) + \nabla\cdot(\mathbf{u}(\mathrm{DON}_s + \mathrm{DON}_r)) = F_{DON} \tag{A2}$$

where $\mathbf{u}$ is the three-dimensional velocity field, DON_s and DON_r are the semi-labile and refractory forms of dissolved organic nitrogen, and F represents the sources and sinks of NO_3^- and DON; full details and explanations are given in *Roussenov et al.* [2005]. *a) Within the euphotic zone* The nitrate source/sink is given in (A1) by

$$F_{NO3} = -G + \beta_s DON_s + \beta_r DON_r, \tag{A3}$$

representing a loss from consumption of nitrate and a supply from the conversion of DON. The consumption of nitrate is given by

$$G = \alpha\left(\frac{I}{I+I_o}\right)\left(\frac{\mathrm{NO}_3^-}{\mathrm{NO}_3^- + \mathrm{NO}_3^-{}_o}\right),$$

where α is the consumption rate, I is the intensity of radiation and $\mathrm{NO}_3^-{}_o$ is the nitrate concentration within the euphotic zone; here, $\alpha = 1\times10^{-6}\mu$M s^{-1}, $I_o = 10$ W m^{-2} and $\mathrm{NO}_3^-{}_o = 1.5\mu$M.

This consumption of nitrate leads to the formation of organic matter with a fraction a_{PON} converted to sinking PON, while the remainder forms DON advected by the flow. The partitioning between PON and DON formation varies with the background nitrate concentrations: the fraction of PON formed, a_{PON}, is 0.5 in nitrate-rich environment ($\mathrm{NO}_3^- > 5\mu$M), but otherwise only 0.2 in nitrate-poor environment. When DON is formed from consumption of nitrate, a fraction of 0.4 is assumed to form semi-labile DON, while the remainder is assumed to form refractory DON.

The DON source/sink in (A2) is given by

$$F_{DON} = (1-a_{PON})G - \beta_s DON_s - \beta_r DON_r, \tag{A4}$$

where there is formation from the consumption of nitrate, as well as a loss from the conversion of semi-labile and refractory DON, which are assumed to occur on timescales of $\beta_s^{-1} = 6$ months and β_r^{-1} 6 to 12 years; the breakdown of DON$_r$ is assumed to occur photochemically and varies with irradience.

b) Below the euphotic zone The PON fallout flux is assumed to exponentially decay with depth below the euphotic zone (assumed to have a thickness $h_e = 100$ m) down to the top of the densest model interface,

$$F(z) = F(-h_e)\exp(\gamma(z + h_e)), \quad \text{(A5)}$$

with a remineralisation depth scale given by $\gamma^{-1} = 200$ m and the flux assumed to vanish at the seafloor, so that there is no loss term of nutrients within the water column. The downwards particulate flux is defined by $F(-h_e) = a_{PON}\int_{z=-h_e}^{z=0} G(z)dz$ at the base of the euphotic zone. Within the interior, nitrate is formed from the remineralisation of PON and from the conversion of semi-labile DON in (A1),

$$F_{NO3} = \frac{\partial F}{\partial z} + \beta_s DON_s, \quad \text{(A6)}$$

while the semi-labile DON is assumed to decay in the interior, but the refractory DON to remain conserved, such that in (A2),

$$F_{DON} = -\beta_s DON_s. \quad \text{(A7)}$$

REFERENCES

Bleck, R. and L. T. Smith, A wind-driven isopycnic coordinate model of the North and Equatorial Atlantic Ocean. 1. Model development and supporting experiments. *J. Geophys. Res., 95,* 3273–3285, 1990.

Broecker, W. S. and T.-H. Peng, Tracers in the Sea, Lamont-Doherty, Columbia University, 690pp, 1982.

Conkright, M. E., S. Levitus and T. P. Boyer, *World Ocean Atlas 1994 volume 1: nutrients*, NOAA Atlas NESDIS 1, U.S. Dept. of Commerce, Washington D.C., 150 pp, 1994.

Glover, D. M., and P. G. Brewer, Estimates of wintertime mixed layer nutrient concentrations in the North Atlantic. *Deep-Sea Res.*, **35**, 1525–1546, 1988.

Gruber, N. and J. L. Sarmiento, Global patterns of marine nitrogen fixation and denitrification, *Global Biogeochem. Cycles, 11*, 235-266, 1997.

Hansell, D. and M. J. Follows, Nitrogen in the Atlantic Ocean, in 'Nitrogen in the Marine Environment', eds. D. Capone, D. Bronk, M. Mulholland, E.Carpenter, submitted, 2005.

Isemer, H. J. and L. Hasse, *The Bunker Climate Atlas of the North Atlantic Ocean*, Vol 2. Springer-Verlag, 252 pp, 1987.

Jenkins, W. J. and S. C. Doney, The subtropical nutrient spiral. *Global Biogeochem. Cycles, 17*, 1110, doi:10.1029/2003GB002085, 2003.

Levitus, S., *Climatological Atlas of the World Ocean*. NOAA prof. Paper No. 13, Washington D.C., 173 pp, 1982.

Mahaffey, C., R.G. Williams, G.A. Wolff and W. Anderson, The physical supply of nutrients to phytoplankton in the Atlantic. *Global Biogeochem. Cycles, 18*, GB1034 10.1029/2003GB002129, 2004.

Marshall, J. C., A. J. G. Nurser and R. G. Williams, Inferring the subduction rate and period over the North Atlantic. *J. Phys. Oceanogr., 23*, 1315-1329, 1993.

McGillicuddy, D.J., A.R. Robinson, D.A. Siegel, H.W. Jannasch, R. Johnson, T. Dickeys, J. McNeil, A.F. Michaels and A.H. Knap, New evidence for the impact of mesoscale eddies on biogeochemical cycling in the Sargasso Sea. *Nature, 394*, 263-266, 1998.

Najjar, R. G., J. L. Sarmiento and J. R. Toggweiler, Downward transport and fate of organic matter in the ocean: simulations with a general circulation model. *Global Biogeochem. Cycles, 6*, 45-76, 1992.

Palter, J. B., M. S. Lozier and R. T. Barber, The impact of advection on the nutrient reservoir in the North Atlantic subtropical gyre. *Nature*, in press, 2005.

Pelegri, J. L. and G. T. Csanady, Nutrient transport and mixing in the Gulf Stream. *J. Geophys. Res., 96*, 2577-2583, 1991.

Pelegri, J. L. and G. T. Csanady, Diapycnal mixing in western boundary currents, *J. Geophys. Res., 99*, 18275–18304, 1994.

Pelegri, J. L., G. T. Csanady and A. Martins, The North Atlantic Nutrient Stream. *J. Oceanogr., 52, 275-299*, 1996.

Rintoul, S., Nutrient return by the Southern ocean overturning circulation: efficacy, pathways and sensitivity to change. Abstract, ASLO Summer meeting, June 19-24, Santiago de Compostela, Spain, 2005.

Rintoul, S.R. and C. Wunsch, Mass, heat, oxygen and nutrient fluxes and budgets in the North Atlantic Ocean. *Deep-Sea Res. I, 38*, S355-S377, 1991.

Roussenov, V., R.G. Williams, C. Mahaffey and G.A. Wolff, Does the transport of dissolved organic nitrogen affect export production in the Atlantic Ocean? *Global Biogeochem. Cycles*, submitted, 2005.

Sarmiento, J. L., N. Gruber, M. A. Brzezinski and J. P. Dunne, High-latitude controls of thermocline nutrients and low latitude biological productivity. *Nature, 427*, 56–60, 2004.

Usbeck, R., R. Schlitzer, G. Fisher and G. Wefer, Particle fluxes in vthe ocean: comparison of sediment trap data with results from inverse modelling. *J. Mar. Sys., 39*, 167-183, 2003.

Valdiviesio da Costa, M., H. Mercier and A. M. Treguier, Effects of the mixed layer time variability on kinematic subduction rate diagnostics. *J. Phys. Oceanogr., 35*, 427–443, 2005.

Williams R. G. and M. J. Follows, The Ekman transfer of nutrients and maintenance of new production over the North Atlantic. *Deep-Sea Res. I, 45*, 461-489, 1998.

Williams, R. G. and M. J. Follows, Physical transport of nutrients and the maintenance of biological production, 19-51, In *'Ocean Biogeochemistry: The role of the ocean carbon cycle in global change',* edited by M. Fasham, Springer, ISBN: 3-540-42398-2, 2003.

Williams, R.G., A. McLaren and M.J. Follows, Estimating the convective supply of nitrate and implied variability in export production. *Global Biogeochem. Cycles, 14*, 1299-1313, 2000.

Table 1. Diagnostics of volume (Sv) and nitrate (kmol s^{-1}) area-integrated fluxes in different density classes for subduction and induction regions over the North Atlantic, as well as nutrient stream diagnostics at 36°N by *Pelegri et al.* [1996]. The subduction and induction estimates are based on diagnostics from 5°N to 60°N over the Atlantic.

σ range	Subduction ($S_{ann} > 0$)		Induction ($S_{ann} < 0$)		Nutrient Stream by *Pelegri et al.* [1996]	
	$\int S_{ann} dA$, $\int S_{ann} N_w dA$		$\int -S_{ann} dA$, $\int -S_{ann} N_w dA$		$\int v dx dz$, $\int v N dx dz$	
	Sv	kmol s^{-1}	Sv	kmol s^{-1}	Sv	kmol s^{-1}
$25.6 \leq \sigma < 26.2$	9.2	24	6.0	13	6.6	44
$26.2 \leq \sigma < 26.5$	7.3	22	5.0	23	8.0	59
$26.5 \leq \sigma < 26.8$	4.2	29	5.7	31	12.5	155
$26.8 \leq \sigma < 27.1$	1.9	18	8.2	89	11.7	219
$27.1 \leq \sigma < 27.3$	2.3	22	4.5	68	5.0	113
$27.3 \leq \sigma < 27.5$	1.7	18	4.0	60	3.6	87
Totals						
$26.5 \leq \sigma < 27.3$	8.4	69	18.4	188	29.2	487
$25.6 \leq \sigma < 27.5$	26.6	133	33.4	284	47.4	677

Figure Captions

Fig. 1. Diagnostics of how the Gulf Stream acts as a 'Nutrient Stream': a) dashed lines depict the boundaries of the 'nutrient stream' and full lines depict the hydrographic sections used in the analysis; b) velocity and nitrate flux with depth along 36°N; c) nitrate flux with density along 36°N. Reproduced from *Pelegri and Csanady* [1991] and *Pelegri et al.* [1996].

Fig. 2. A schematic figure of how fluid and nutrients are transferred from the thermocline into the mixed layer: (a) a meridional section where a particle moves with a velocity velocity, w, and a horizontal velocity, $\mathbf{u}$, which leads to both a vertical and lateral transfer into a polewards thickening mixed layer. The shading denotes an isopycnal layer and the dashed line the base of the mixed layer; (b) a three-dimensional view where there is a nutrient stream associated with the western boundary current which ultimately transfers nutrients into the downstream mixed layer. When the nutrients are transferred into the mixed layer, they are vertically redistributed through the convection process. The nutrients can eventually be redistributed to other density layers through the diabatic transfer within the mixed layer or remineralisation of a particle flux.

Fig. 3. Climatological diagnostics of the mixed layer: (a) March mixed-layer depth H (m) from the Levitus climatology (smoothed to remove fine scales); (b) March mixed-layer σ_t with dashed contours covering the σ range of the nutrient stream; (c) nitrate concentration in the mixed layer (μM) in March diagnosed using the interpolation method of *Glover and Brewer* [1988] from climatological nitrate of *Conkright et al.* [1994]; (d) Dynamic height field (m) at the surface relative to 2500 m derived by integrating the thermal-wind equations with the Levitus climatology.

Fig. 4. Climatological diagnostics of the volume flux and associated nitrate flux into the Ekman layer and the seasonal boundary layer: (a) Annual-mean Ekman upwelling, w_{ek} (m y^{-1}) from the Isemer and Hasse (1987) climatology; (b) Annual volume flux into the seasonal boundary layer, $-S_{ann}$ (m y^{-1}); (c) Ekman upwelling flux of nitrate, $w_{ek}N$ (m y$^{-1}\mu$M); (d) Induction flux of nitrate into the seasonal boundary layer, $-S_{ann}N$ (m y$^{-1}\mu$M).

Fig. 5. Climatological diagnostics of the vertical and horizontal components of the annual volume

flux and associated nitrate flux into the seasonal boundary layer: (a) vertical volume flux per unit horizontal area, w_b (m y^{-1}); (b) horizontal volume flux per unit horizontal area, $u_b.\nabla H$ (m y^{-1}); (c) vertical nitrate flux, Nw_b (m y$^{-1}\mu$M); (d) horizontal nitrate flux per unit horizontal area, $Nu_b.\nabla H$ (m y$^{-1}\mu$M).

Fig. 6. Nitrate distributions (μM) from climatology (left panel) and the default model integration (right panel) for (a) meridional section along 25°W and (b) maps of nitrate concentration in the upper 100 m, together with model maps for (c) annual export of particulate organic nitrogen (PON) at a depth of 100 m (M m^{-2}y^{-1}) and (d) concentrations of DON (μN) in the upper 100 m.

Fig. 7. Model diagnostics of (a) trajectories and (b) layer streamfunction (Sv) and nitrate concentration (μM) along $\sigma = 27.03$ (and where the layer outcrops, for the mixed layer). In (a), trajectories are integrated for 20 years using a mean velocity field with an initial release at sites A to E. Regions of high nitrate fluxes > 20 kmol s^{-1} over the upper 1500 m are shaded. In the upper right panel, diagnostics are included for the transport in Sv over the upper 1500 m (solid line), the zonally-integrated Nitrate flux in kmol s^{-1} (long dashed line) and the Nitrate flux zonally-integrated over the shaded region marked on the left panel.

Fig. 8. Modelled nutrient stream: (a) vertical sections at 36°N for the northwards velocity (cm s^{-1}), nitrate and DON flux (mM m^{-2}s^{-1}) through the section; (b) σ sections of nitrate flux and DON flux through 36°N; c) nitrate flux through 20°S, 3 °N and 55°N. Shading denotes elevated values and note that a greater contour interval is used for the DON flux.

Fig. 9. Model tracer simulations with a tracer source in the Gulf Stream after a 40 year, online tracer integration and a 60 year dynamical spin up. The tracer is either conserved (left panel) or behaves in the same manner as nitrate (right panel). There are (a) map of the tracer distribution for a tracer release near the Gulf Stream, and (b) meridional sections along 40°W for a tracer release along $\sigma = 26.52$, and repeated in (c) and (d) for a tracer release along $\sigma = 27.03$. In (a) and (c), the dashed line denoted the end of winter outcrop of the mixed layer, while in (b) and (d), the thick and thin dashed lines denote the base of the mixed layer at the end of winter and the interfaces of the layer where the tracer is released.

Fig. 10. Diagnostics of nitrate (left panel) and PO4* (right panel) in μM on (a) $\sigma = 26.5$, (b) $\sigma = 27.0$ and (c) $\sigma = 27.5$ for the Atlantic. Nitrate concentrations greater than 25μM are shaded. Note how the maximum nitrate concentrations occur in the tropics for the lighter surfaces, even though the PO4* tracer denotes a southern source.

Fig. 11. Model tracer simulations with a source on the southern boundary after 40 years, online tracer integration and a 60 year dynamical spin up. Two cases are shown, a conserved tracer with no interior source (left panel) and tracer with an additional source from the remineralisation of a particle flux occurring whenever the tracer from the same layer spreads into the surface mixed layer (right panel): (a) $\sigma = 26.52$, (b) $\sigma = 27.03$. Note how the tracer with a remineralisation source shows a local maximum over the tropics with concentrations exceeding the original source on the southern boundary.

Fig. 12. Schematic figures depicting (a) transfers within the northern subtropical gyre and (b) possible nutrient pathways in the Atlantic. Sub-antarctic mode waters (grey shaded region) is formed in the southeast Pacific with characteristic high nutrient concentrations and low salinity. The mode water is transferred northwards through lateral Ekman and gyre (black) circulations, eventually being subducted as Antarctic Intermediate Water (AAIW). The AAIW is swept northwards as part of the intermediate circulation (grey) with nutrient concentrations significantly enhanced in the tropical upwelling through fallout and remineralisation. This nutrient-rich water is then transferred into the northern basin with the nutrient stream eventually leading to a downstream nutrient influx into the mixed layer.

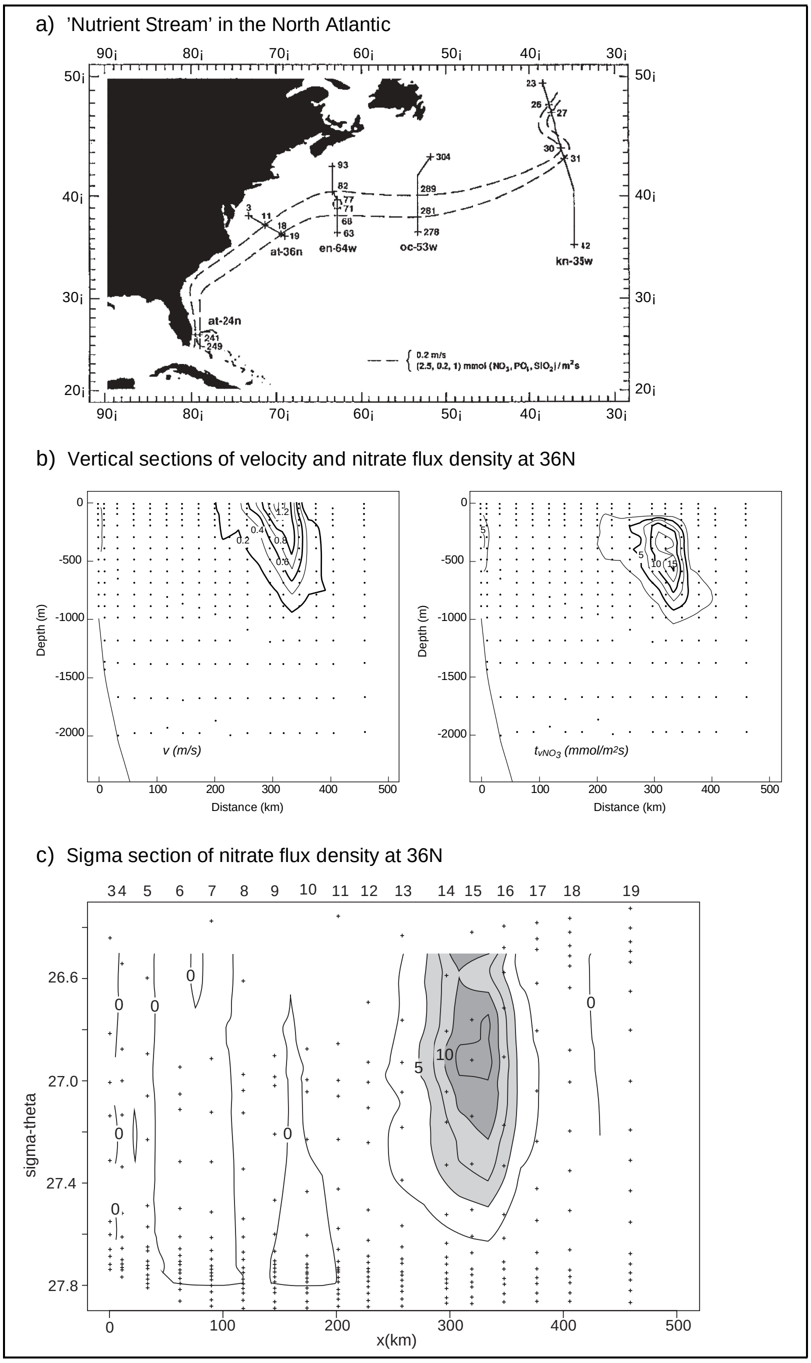

Figure 1: Diagnostics of how the Gulf Stream acts as a 'Nutrient Stream': a) dashed lines depict the boundaries of the 'nutrient stream' and full lines depict the hydrographic sections used in the analysis; b) velocity and nitrate flux with depth along 36°N; c) nitrate flux with density along 36°N. Reproduced from *Pelegri and Csanady* [1991] and *Pelegri et al.* [1996].

a) transfer of fluid from the thermocline to the mixed layer

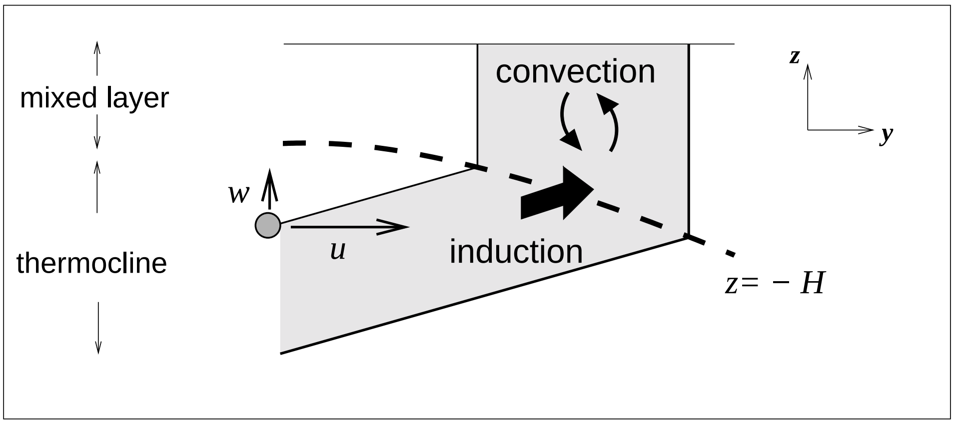

b) nutrient stream and its downstream transfer

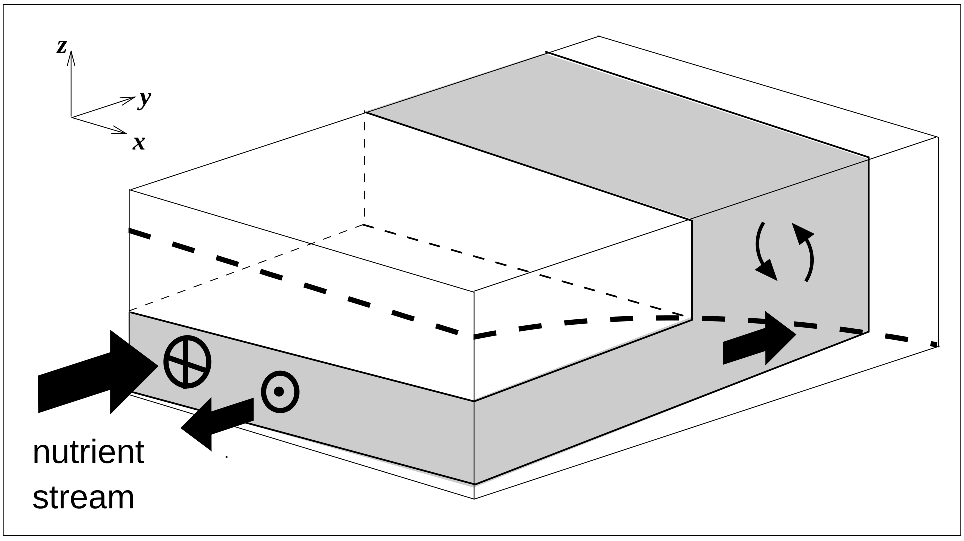

Figure 2: A schematic figure of how fluid and nutrients are transferred from the thermocline into the mixed layer: (a) a meridional section where a particle moves with a velocity velocity, w, and a horizontal velocity, $\mathbf{u}$, which leads to both a vertical and lateral transfer into a polewards thickening mixed layer. The shading denotes an isopycnal layer and the dashed line the base of the mixed layer; (b) a three-dimensional view where there is a nutrient stream associated with the western boundary current which ultimately transfers nutrients into the downstream mixed layer. When the nutrients are transferred into the mixed layer, they are vertically redistributed through the convection process. The nutrients can eventually be redistributed to other density layers through the diabatic transfer within the mixed layer or remineralisation of a particle flux.

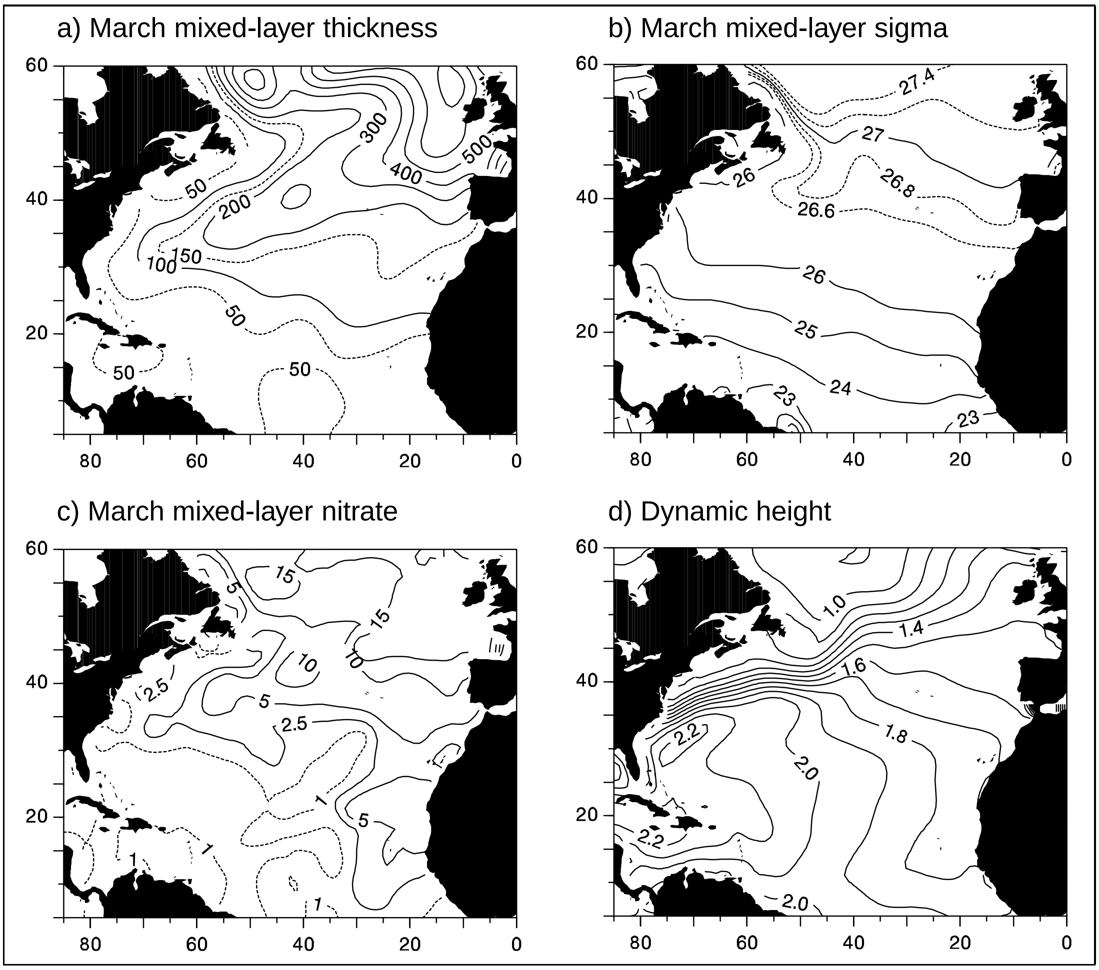

Figure 3: Climatological diagnostics of the mixed layer: (a) March mixed-layer depth H (m) from the Levitus climatology (smoothed to remove fine scales); (b) March mixed-layer σ_t with dashed contours covering the σ range of the nutrient stream; (c) nitrate concentration in the mixed layer (μM) in March diagnosed using the interpolation method of *Glover and Brewer* [1988] from climatological nitrate of *Conkright et al.* [1994]; (d) Dynamic height field (m) at the surface relative to 2500 m derived by integrating the thermal-wind equations with the Levitus climatology.

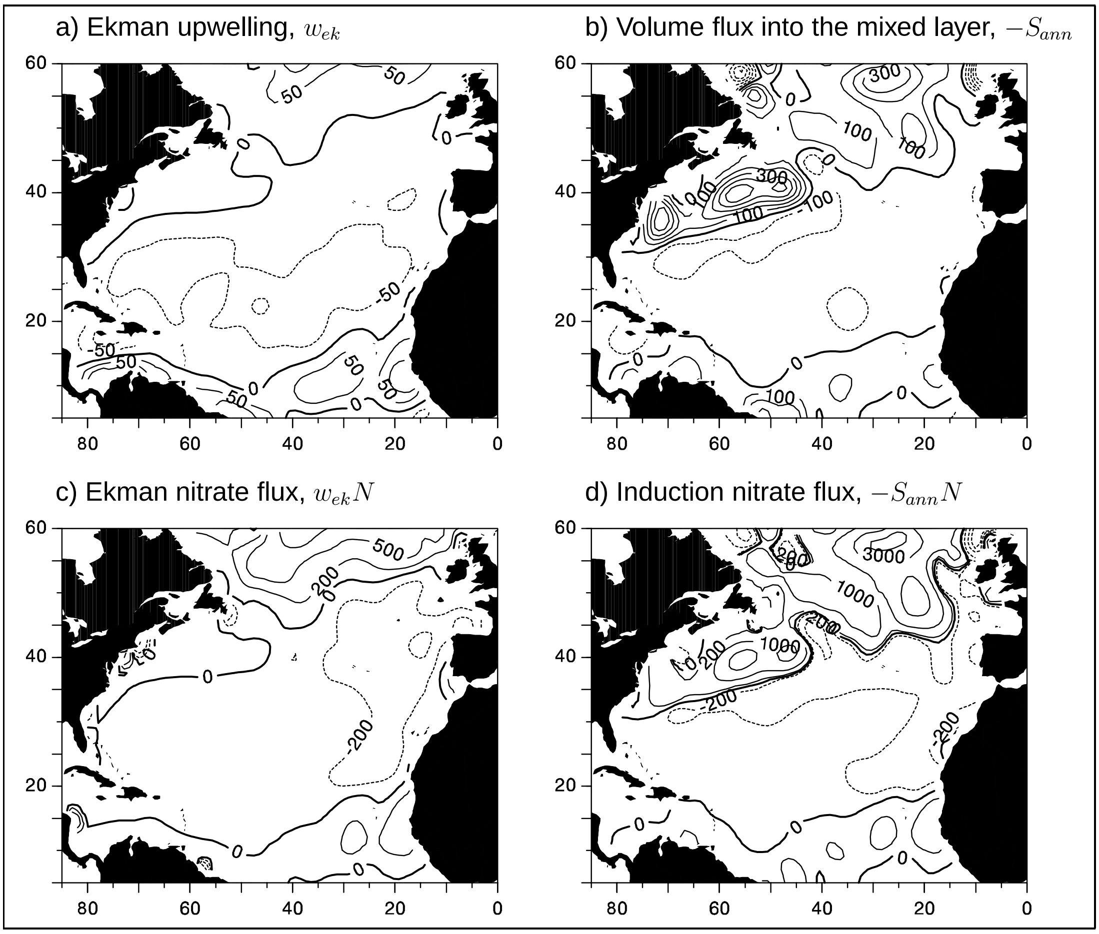

Figure 4: Climatological diagnostics of the volume flux and associated nitrate flux into the Ekman layer and the seasonal boundary layer: (a) Annual-mean Ekman upwelling, w_{ek} (m y^{-1}) from the Isemer and Hasse (1987) climatology; (b) Annual volume flux into the seasonal boundary layer, $-S_{ann}$ (m y^{-1}); (c) Ekman upwelling flux of nitrate, $w_{ek}N$ (m y$^{-1}\mu$M); (d) Induction flux of nitrate into the seasonal boundary layer, $-S_{ann}N$ (m y$^{-1}\mu$M).

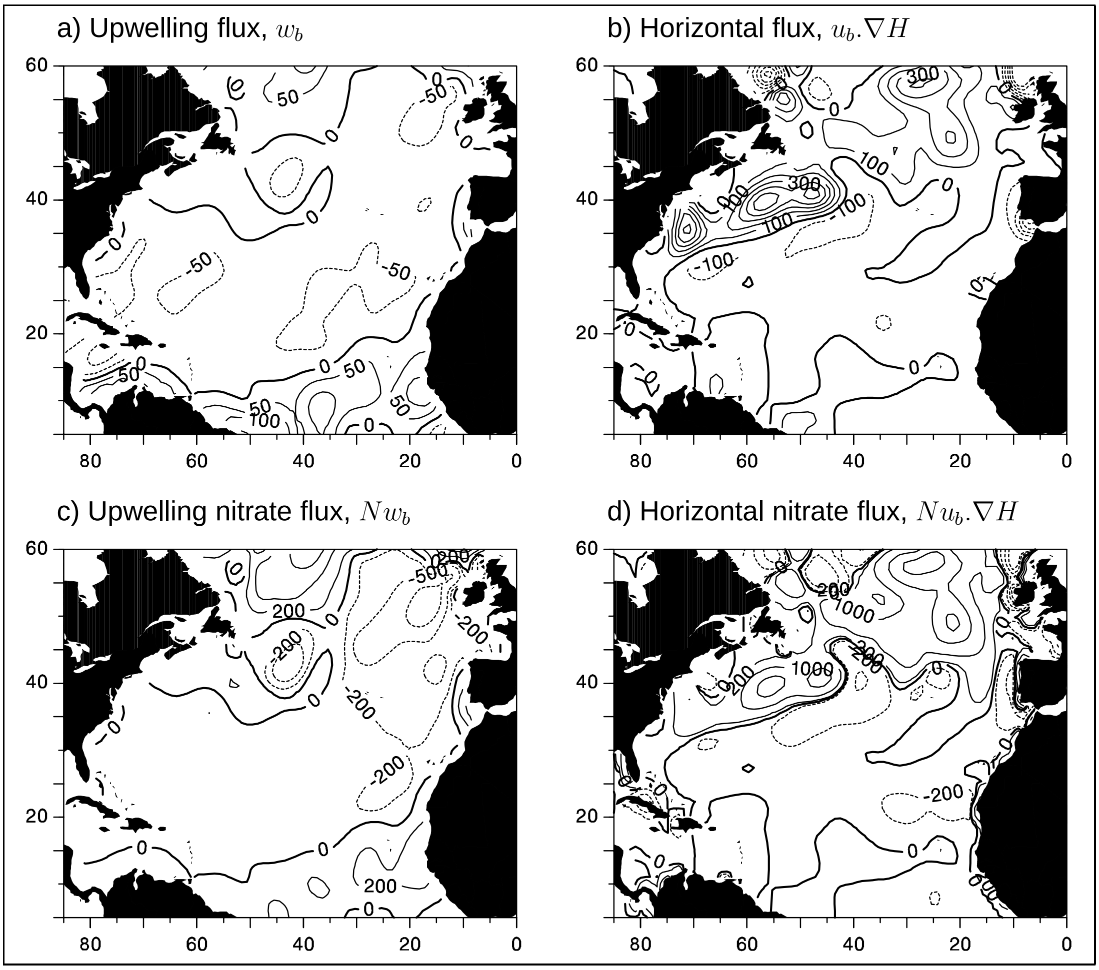

Figure 5: Climatological diagnostics of the vertical and horizontal components of the annual volume flux and associated nitrate flux into the seasonal boundary layer: (a) vertical volume flux per unit horizontal area, w_b (m y^{-1}); (b) horizontal volume flux per unit horizontal area, $u_b.\nabla H$ (m y^{-1}); (c) vertical nitrate flux, Nw_b (m y$^{-1}\mu$M); (d) horizontal nitrate flux per unit horizontal area, $Nu_b.\nabla H$ (m y$^{-1}\mu$M).

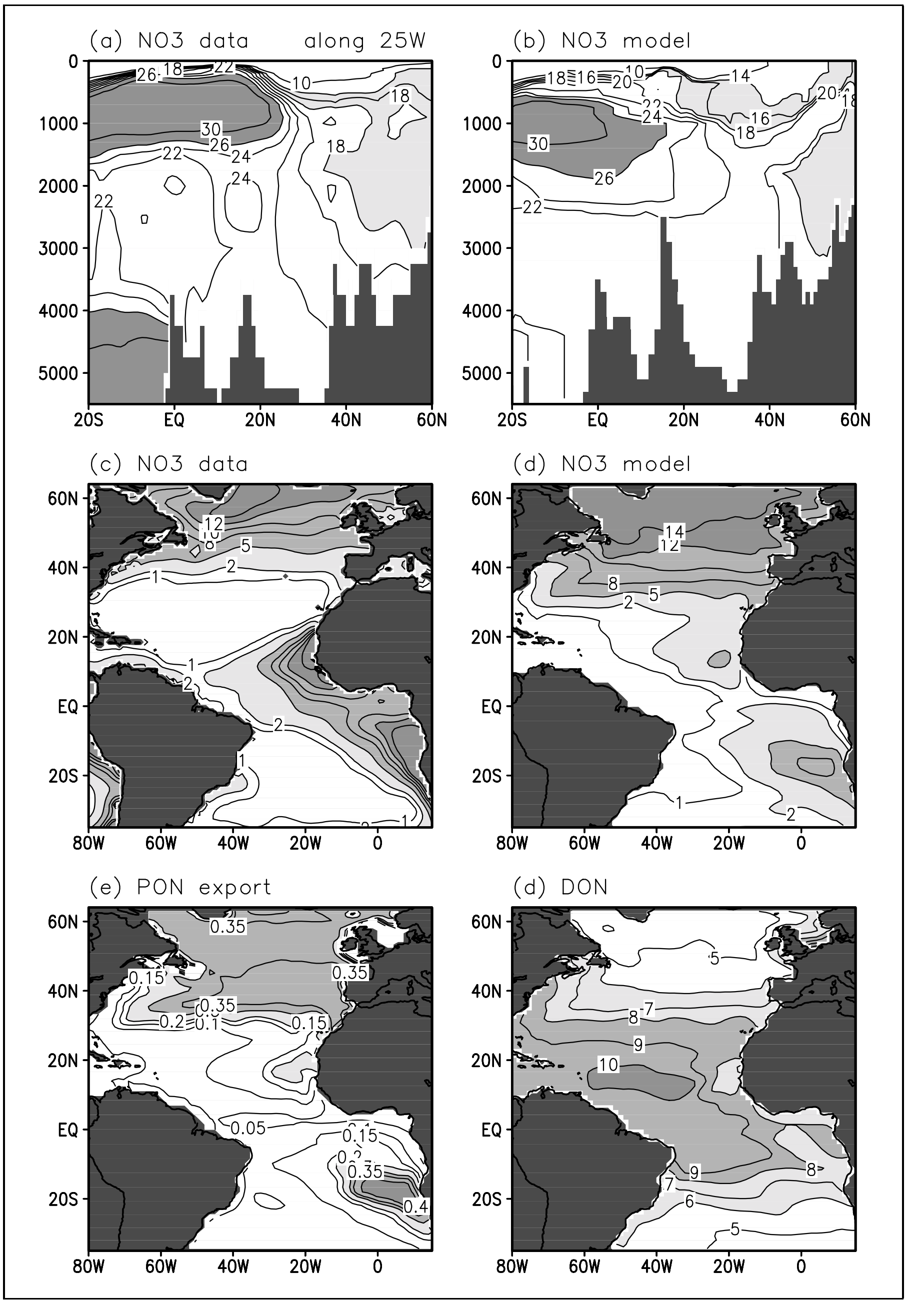

Figure 6: Nitrate distributions (μM) from climatology (left panel) and the default model integration (right panel) for (a) meridional section along 25°W and (b) maps of nitrate concentration in the upper 100 m, together with model maps for (c) annual export of particulate organic nitrogen (PON) at a depth of 100 m (M m^{-2}y^{-1}) and (d) concentrations of DON (μN) in the upper 100 m.

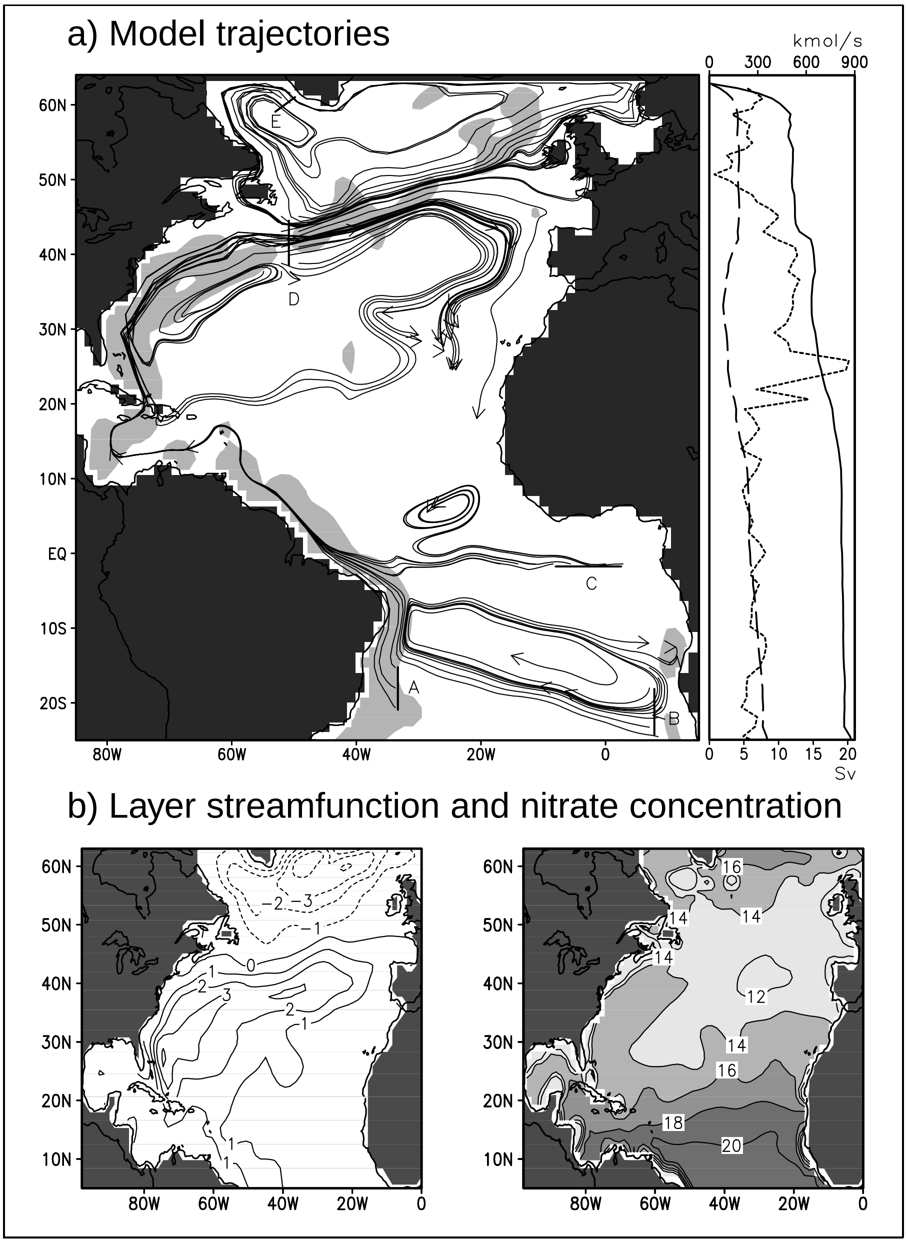

Figure 7: Model diagnostics of (a) trajectories and (b) layer streamfunction (Sv) and nitrate concentration (μM) along $\sigma = 27.03$ (and where the layer outcrops, for the mixed layer). In (a), trajectories are integrated for 20 years using a mean velocity field with an initial release at sites A to E. Regions of high nitrate fluxes > 20 kmol s^{-1} over the upper 1500 m are shaded. In the upper right panel, diagnostics are included for the transport in Sv over the upper 1500 m (solid line), the zonally-integrated Nitrate flux in kmol s^{-1} (long dashed line) and the Nitrate flux zonally-integrated over the shaded region marked on the left panel.

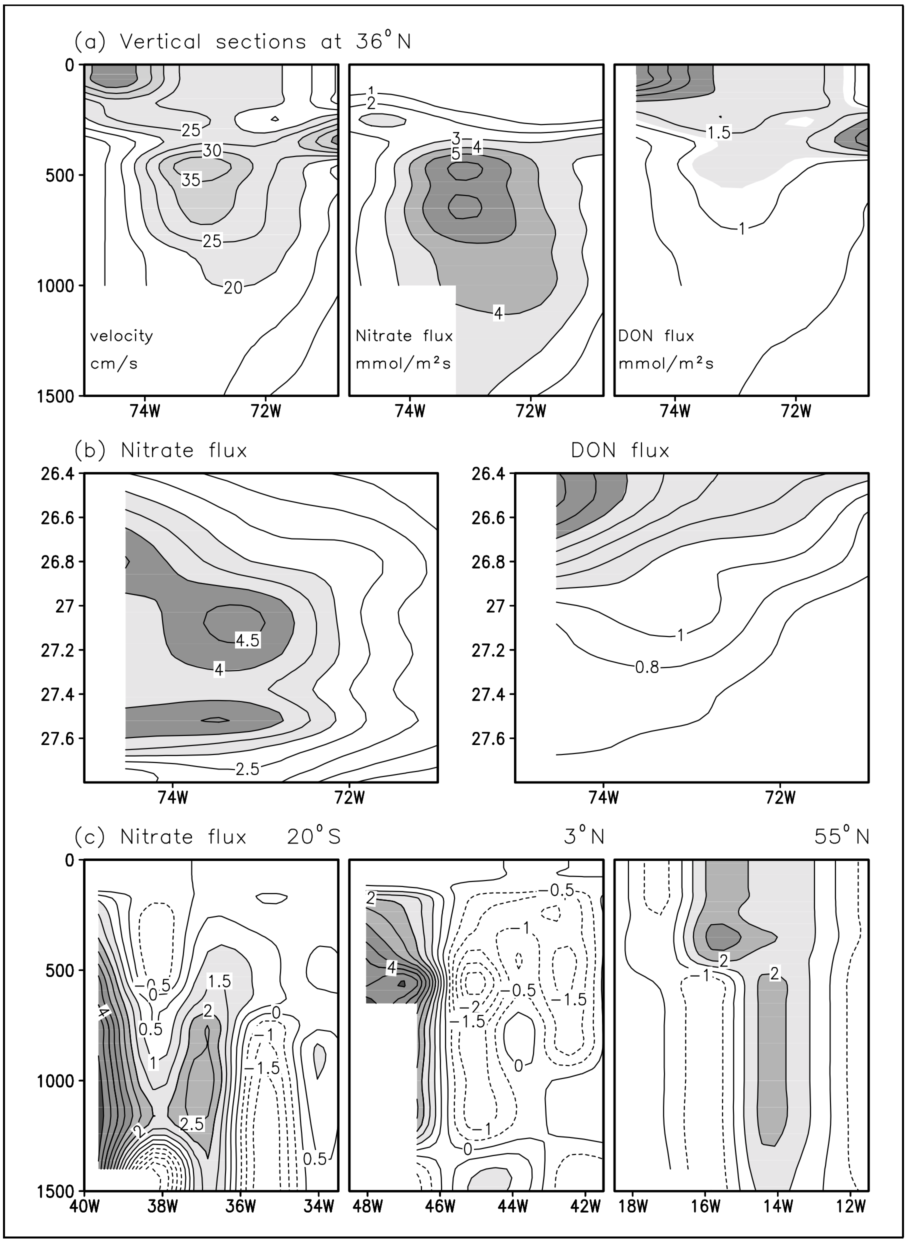

Figure 8: Modelled nutrient stream: (a) vertical sections at 36°N for the northwards velocity (cm s^{-1}), nitrate and DON flux (mM m^{-2}s^{-1}) through the section; (b) σ sections of nitrate flux and DON flux through 36°N; c) nitrate flux through 20°S, 3 °N and 55°N. Shading denotes elevated values and note that a greater contour interval is used for the DON flux.

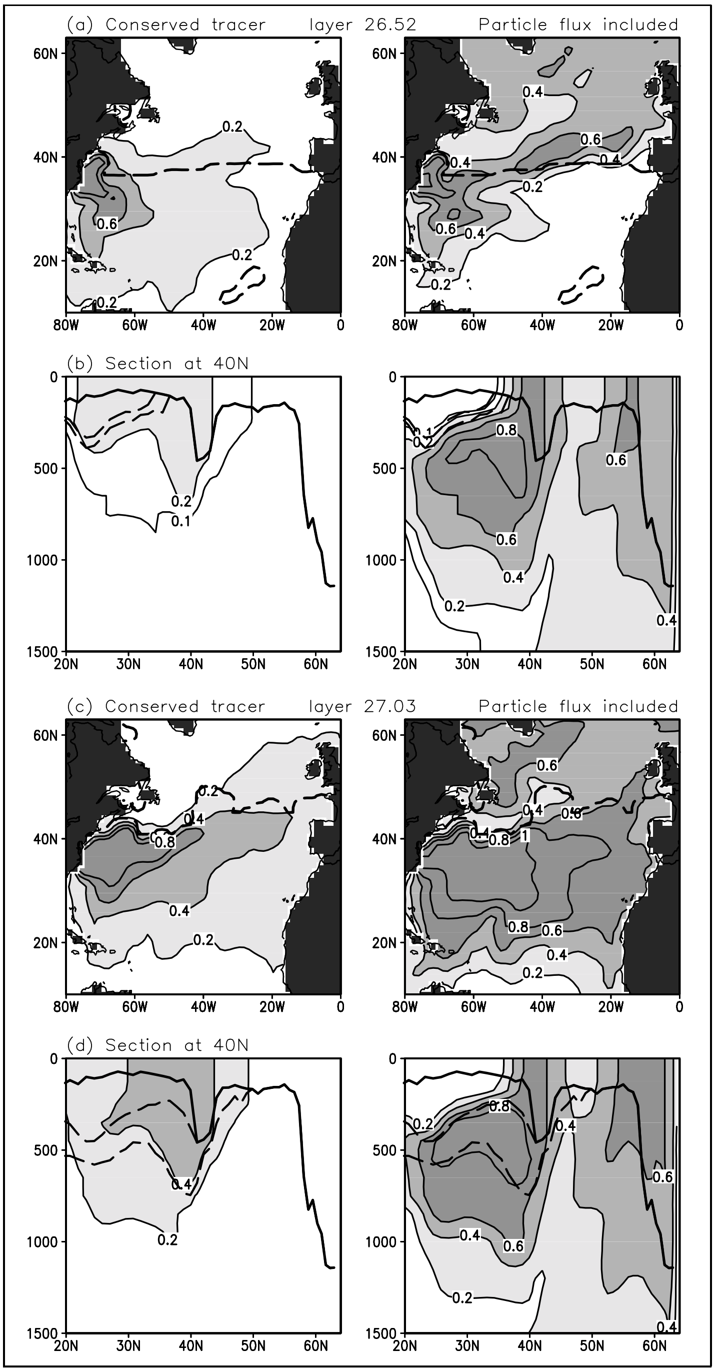

Figure 9: Model tracer simulations with a tracer source in the Gulf Stream after a 40 year, online tracer integration and a 60 year dynamical spin up. The tracer is either conserved (left panel) or behaves in the same manner as nitrate (right panel). There are (a) map of the tracer distribution for a tracer release near the Gulf Stream, and (b) meridional sections along 40°W for a tracer release along $\sigma = 26.52$, and repeated in (c) and (d) for a tracer release along $\sigma = 27.03$. In (a) and (c), the dashed line denoted the end of winter outcrop of the mixed layer, while in (b) and (d), the thick and thin dashed lines denote the base of the mixed layer at the end of winter and the interfaces of the layer where the tracer is released.

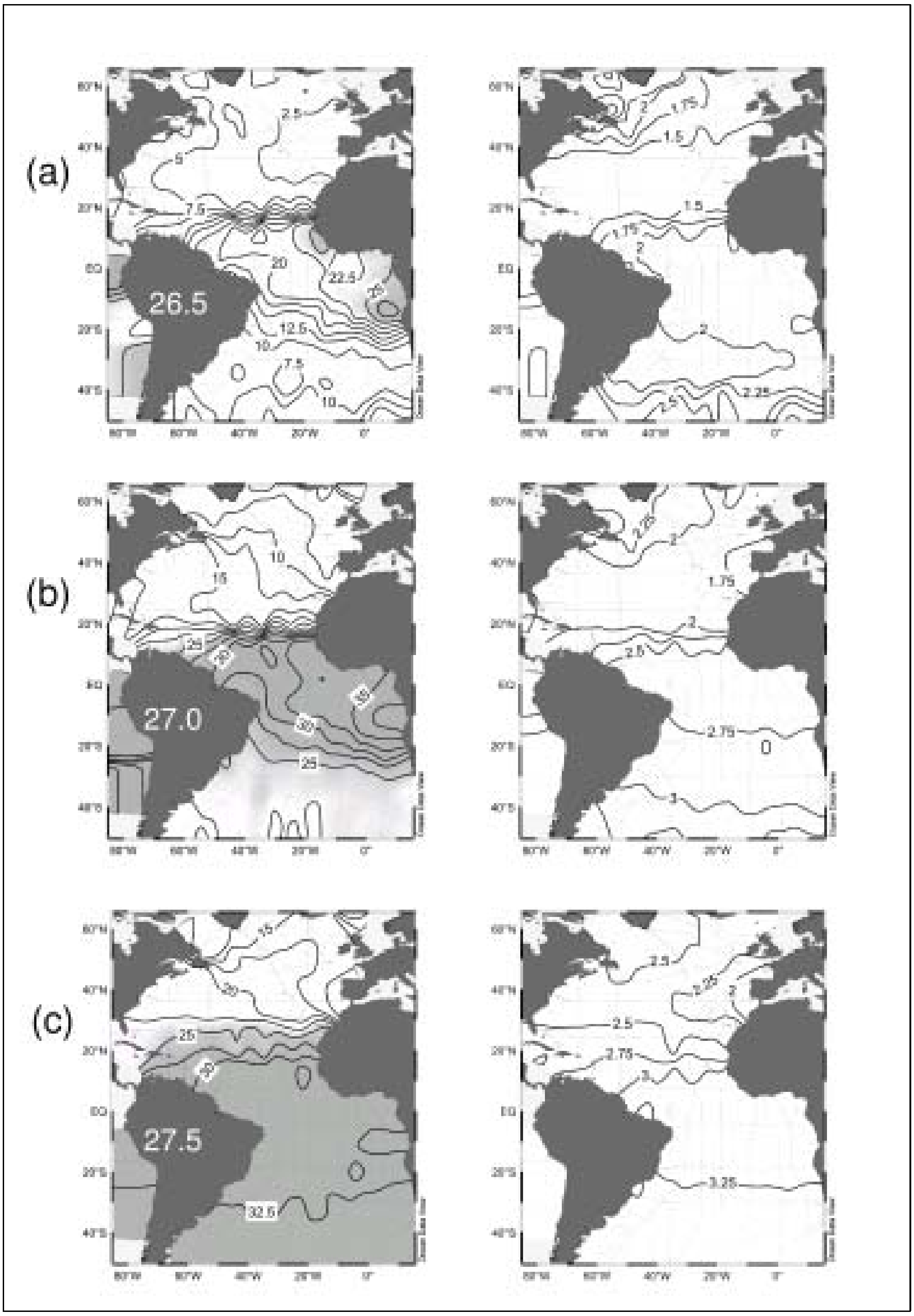

Figure 10: Diagnostics of nitrate (left panel) and PO4* (right panel) in μM on (a) $\sigma = 26.5$, (b) $\sigma = 27.0$ and (c) $\sigma = 27.5$ for the Atlantic. Nitrate concentrations greater than 25μM are shaded. Note how the maximum nitrate concentrations occur in the tropics for the lighter surfaces, even though the PO4* tracer denotes a southern source.

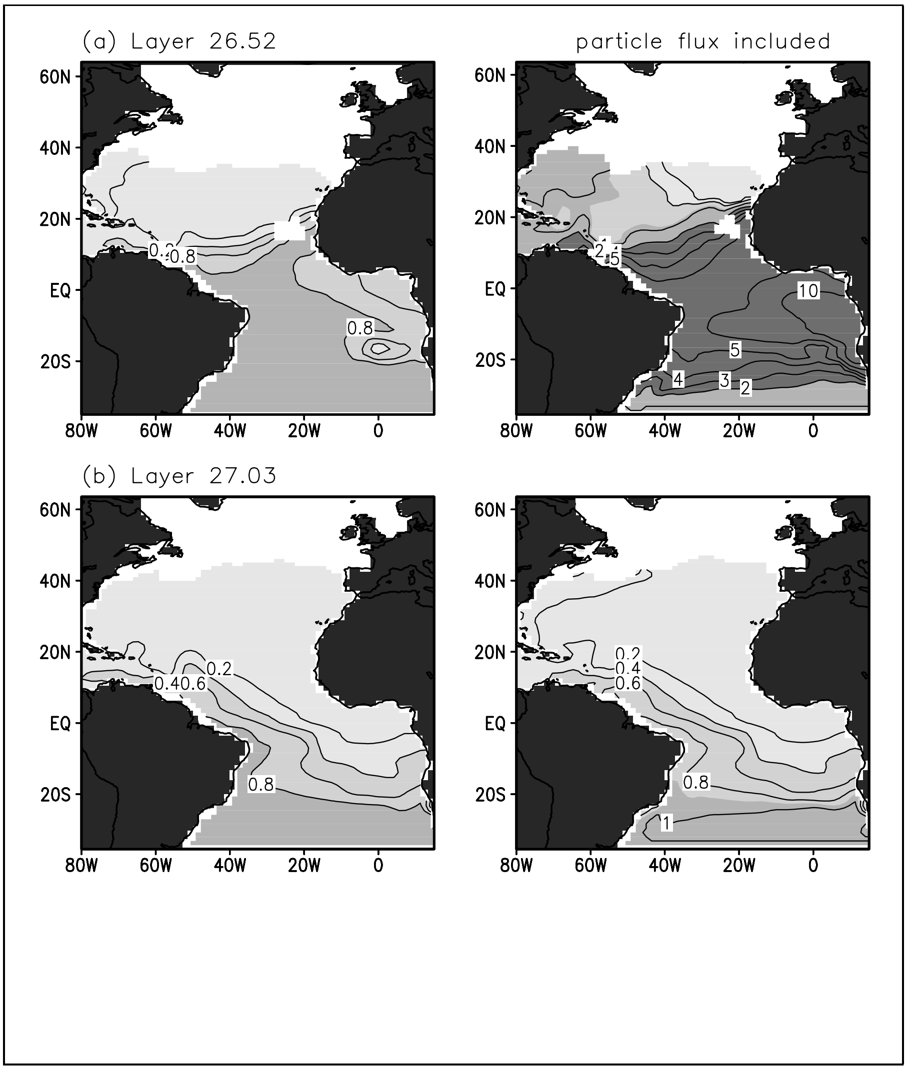

Figure 11: Model tracer simulations with a source on the southern boundary after 40 years, online tracer integration and a 60 year dynamical spin up. Two cases are shown, a conserved tracer with no interior source (left panel) and tracer with an additional source from the remineralisation of a particle flux occurring whenever the tracer from the same layer spreads into the surface mixed layer (right panel): (a) $\sigma = 26.52$, (b) $\sigma = 27.03$. Note how the tracer with a remineralisation source shows a local maximum over the tropics with concentrations exceeding the original source on the southern boundary.

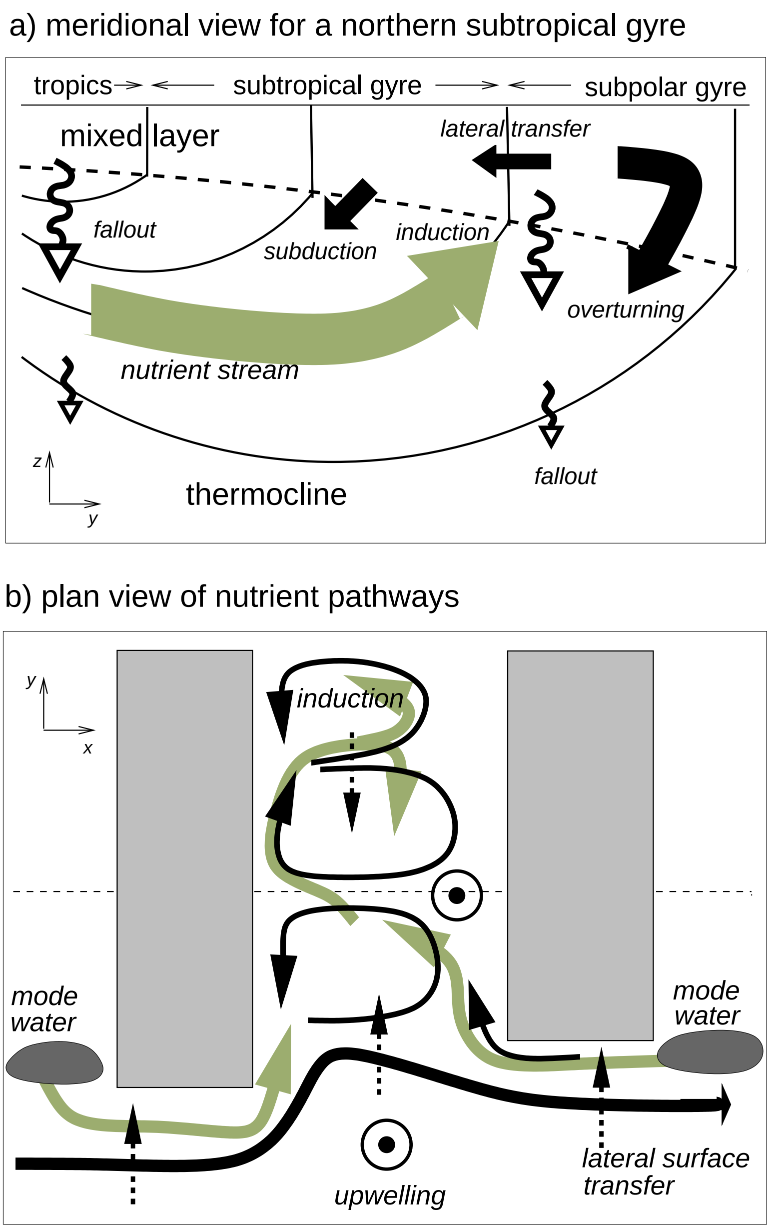

Figure 12: Schematic figures depicting (a) transfers within the northern subtropical gyre and (b) possible nutrient pathways in the Atlantic. Sub-antarctic mode waters (grey shaded region) is formed in the southeast Pacific with characteristic high nutrient concentrations and low salinity. The mode water is transferred northwards through lateral Ekman and gyre (black) circulations, eventually being subducted as Antarctic Intermediate Water (AAIW). The AAIW is swept northwards as part of the intermediate circulation (grey) with nutrient concentrations significantly enhanced in the tropical upwelling through fallout and remineralisation. This nutrient-rich water is then transferred into the northern basin with the nutrient stream eventually leading to a downstream nutrient influx into the mixed layer.